Vibrational Spectra of Some Carotenoids and Related Linear Polyenes. A Raman Spectroscopic Study

L. Rimai,* M. E. Heyde, and D. Gill

Contribution from the Scientific Research Staff, Ford Motor Company, Dearborn, Michigan 48121. *Received February 17, 1973*

Abstract: The vibrational resonance Raman (RR) spectra of β-carotene and its synthetic homologs $C_{30}H_{44}$, $C_{35}H_{50}$, $C_{50}H_{68}$, and $C_{60}H_{80}$ of bixin, crocetin, capsanthin, the polyene antibiotic Amphotericin B (Fungizone), and of deuterio-β-carotene are presented. The spectra of bixin and crocetin, which are carotenoid chains stripped of ionone rings, are similar to those of β-carotene; thus the conjugated chain is identified as the main contributor to the RR spectra of all carotenoids. A theoretical model of in-plane vibrations in an infinitely long polyvinylene chain is used to prove that: (a) the frequency of the intense ethylenic mode at $\sim$1500 cm^{-1} is a genuine measure of the stiffness of the C=C bonds (hence the frequency of the ethylenic mode is an indicator of bond alternation) and (b) the band at 1100–1200 cm^{-1} results from the admixture of C—C and C=C stretching with C—H bending, explaining why the observed frequency does not increase with the stiffening of the C—C bonds in the chain. For deuterio carotenoids the model calculation yields much less satisfactory mode assignments. Possible implications of this result are discussed.

The Raman spectra of organic molecules containing extended linear-conjugated sections are usually very intense due to the phenomenon of resonance enhancement.[1-4] Thus, spectra of natural carotenoid pigments can be easily obtained from dilute solutions (μM concentrations)[3] and from intact tissue samples.[5,6] The vibrational Raman spectra are useful for the characterization of molecular configuration and state of binding, as shown particularly for the stereoisomers of retinal.[7] In order to better utilize this information, especially with regard to details of molecular geometry, it is important to achieve reasonable understanding of the molecular dynamics involved. We report here on a Raman spectroscopic survey of normal and deuterio-β-carotene, of other natural carotenoids, and of a series of synthetic β-carotene homologs with various chain lengths. The data are discussed in terms of a theoretical model which, even if oversimplified and approximate, provides solid ground for understanding the vibrational spectra of a whole class of polyene molecules in terms of a small number of physically meaningful parameters. Thus, for example, it is applicable to the polyvinylene chromophores in Type K Polaroid sheets,[8] to the polyene segment of the antibiotic Amphotericin B (Fungizone),[9] as well as to the stereoisomers of retinal. Specifically, the model seems to account reasonably for the features of the Raman spectra of all the protonated carotenoid molecules. Its failure with respect to the deuterio carotenoids is also reported and discussed.

(1) J. Behringer in "Raman Spectroscopy," Vol. 1, H. A. Szymanski, Ed., Plenum Press, New York, N. Y., 1967, Chapter 6.
(2) T. M. Ivanova, L. A, Yanovskaya, and P. P. Shorygin, *Opt. Spectrosc. (USSR)*, **18**, 115 (1965).
(3) L. Rimai, R. G. Kilponen, and D. Gill, *J. Amer. Chem. Soc.*, **92**, 3824 (1970).
(4) M. C. Hutley and D. J. Jacobs, *Chem. Phys. Lett.*, **6**, 269 (1970).
(5) D. Gill, R. G. Kilponen, and L. Rimai, *Nature (London)*, **227**, 743 (1970).
(6) L. Rimai, R. G. Kilponen, and D. Gill, *Biochem. Biophys. Res. Commun.*, **41**, 492 (1970).
(7) D. Gill, M. E. Heyde, and L. Rimai, *J. Amer. Chem. Soc.*, **93**, 6288 (1971).
(8) D. Gill, R. G. Kilponen, and L. Rimai, *Chem. Phys. Lett.*, **8**, 634 (1971).
(9) P. Ganis, G. Avitabile, W. Mechlinski, and C. P. Schaffner, *J. Amer. Chem. Soc.*, **93**, 4560 (1971).

Vibrational Model

The simplified model for the molecular dynamics of the carotenoids and polyenes is based on the infinite periodic structure approximation.[10] It seems to be well established that the most intense lines in the Raman spectra of these compounds are due to modes strongly coupled to the conjugated molecular skeleton and which involve a substantial contribution from the C=C bond stretching deformations.[4,6,8] For example, the spectra of bixin and crocetin, which have no terminal rings, are very similar to that of β-carotene (Figure 1). Therefore, the hydrocarbon backbone in these compounds can be approximated by a polyvinylene molecule consisting of a sequence of 7 to 20 identical repeat units each containing a pair of carbon atoms, one double and one single bond, and a pair of allylic protons (Figure 2). The presence of the CH_3 side groups (Figure 3) will not significantly alter the frequencies of the modes involving the chain carbons and protons (compare data on carotenoids, Amphotericin B, and Polaroid K sheet).[8] The methyl groups are, however, responsible for an additional line at about 1010 cm^{-1}, corresponding to the stretching of the C–CH_3 bond perpendicular to the molecular axis. The approximation is further justified by the manner in which it is used; rather than attempting the complete quantitative fitting to the experimental data, the model is used to examine trends as a function of systematic variations in the initial dynamic parameters. Thus it enables one to make reasonable assignments of lines or groups of lines to modes involving combinations of given dynamic internal coordinates. The present discussion is more general than previous treatments of the infinite periodic model for polyenes[10] in that it explicitly includes the in-plane proton–carbon bending deformations. (These have, however, been included in recent calculations of finite chains.[11]) This inclusion is very essential to the understanding of the spectra, as the quasidegeneracy of the respective frequencies in protonated polyenes causes a strong admixture of C–H bending with C–C stretching deformations. Furthermore, orthogonality conditions

(10) C. Tric, *J. Chem. Phys.*, **51**, 4778 (1969).
(11) R. M. Gavin and S. A. Rice, *J. Chem. Phys.*, **55**, 2675 (1971).

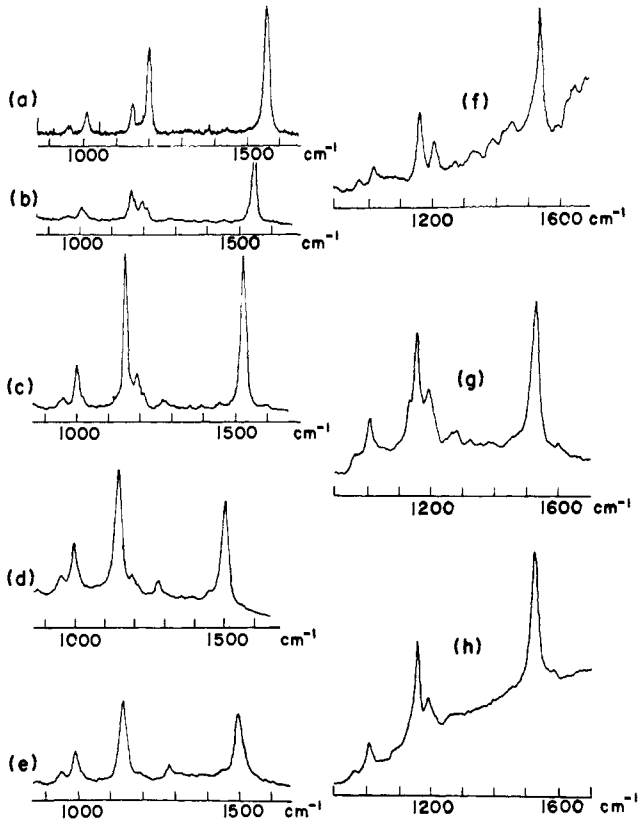

Figure 1. Raman spectra of various carotenoids (notation in Figure 3). (a–e) Synthetic homologs of β-carotene in CCl_4 solution: (a) (2,1|1,2), $C_{30}H_{44}$, (b) (2,1|2,2), $C_{35}H_{50}$, (c) (2,2|2,2), $C_{40}H_{58}$ β-carotene, (d) $C_{50}H_{68}$ (2,3|3,2), (e) $C_{60}H_{80}$ (2,4|4,2) (The spectra are not superimposed because of differences in the frequency scale. Noteworthy length-dependent trends: the lowering of ν(C=C) from above to below 1500 cm^{-1}, the alternation of intensities at 1160 and 1200 cm^{-1}, the emergence of a peak below 1300 cm^{-1}.); (f) crocetin (48.1|1,48) in ethanol, excited at 488.0 nm; (g) bixin (44,2|2,45) in ethanol, excited at 514.5 nm. The stereoisomer is unknown. The analogy of a to e with f and g identifies the conjugated chain as the sole source of the spectra. The intensity distribution near ~1200 cm^{-1} shows the same length-dependent trend from f to g like the one from b to c. (h) Capsanthin, in a crude extract of paprika, redissolved in CCl_4 and excited at 514.5 nm. It is distinct from the spectrum of β-carotene in ν(C=C) (5 cm^{-1} below that of β-carotene) and in the absence of weak lines.

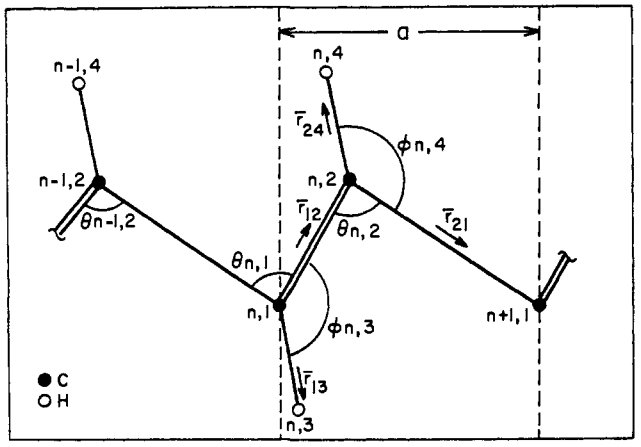

Figure 2. In-plane internal coordinates of the nth unit cell of polyvinylene $(-CH{=}CH-)_n$. Equilibrium bond lengths: C=C 1.337 Å, C—C 1.483 Å, C—H 1.082 Å; angles $2\pi/3$. Notation for deformations:[10,13] stretching, Q for C=C, Q_0 for C—C, q for C—H; in-plane bending, γ for C—C=C, β for C=C—H and also for C—C—H.

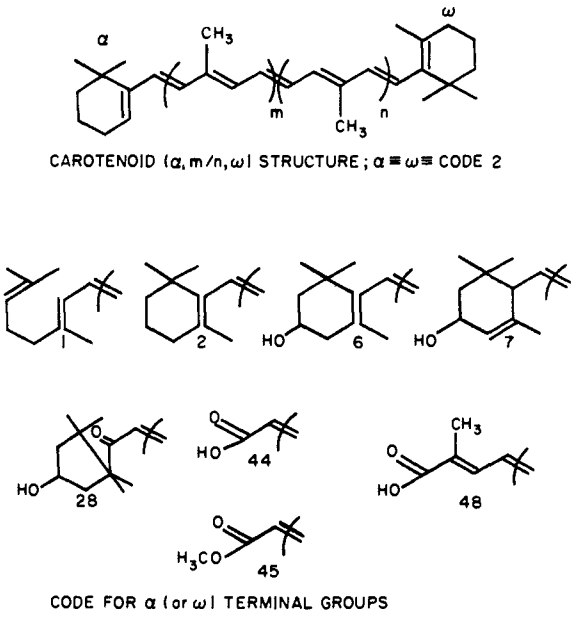

Figure 3. Schematic presentation of carotenoid polymers. The conjugated chain consists of a m-oligomer and a n-oligomer of the repeat unit connected head to head. The bracket boundaries of the "large" (isoprenoid or carotenoid) repeat unit enclose two double bonds in a way consistent with the monomer precursor. Each terminal group has a half integral number of double bonds. The $(\alpha,m|n,\omega)$ notation covers the α and ω terminal groups and the m- and n-oligomers. The number code for the terminal groups is conventional, although the bracket boundaries are shifted so as to match integral numbers of repeat units. In this notation β-carotene reads (2,2|2,2) and its synthetic homologs are $(2,m|n,2)$, lycopene is (1,2|2,1), lutein (6,2|2,7), zeaxanthin (6,2|2,6), crocetin (48,1|1,48), bixin (44,2|2,45), and capsanthin (6,2|2,28). In summing the conjugated double bonds, distinction should be made between chain bonds and contiguous double bonds located in the ionone rings. Thus, β-carotene has $2(m + n) + 1/2 + 1/2 = 9$ chain bonds + 2 ring bonds, while lycopene has 11 conjugated double bonds in a linear chain.

force the admixture of C=C stretching into these already mixed modes. The importance of the C=C stretching admixture is in its contribution to the resonance enhancement of the intensity of the mode.

The infinite chain model permits band assignments to be made independent of chain length, while the frequencies of individual modes within the bands are determined by the length of the molecule.

For planar molecules (such as the conjugated backbone of unstrained carotenoid isomers) the normal vibrations subdivide into two mutually orthogonal subsets: the in-plane and the out-of-plane modes. In a linear theory one has an independent system of dynamic equations for each subset. Since all the observed Raman lines have diagonal scattering tensors (polarized modes), which is an inherent property of the in-plane vibrations, we restrict the discussion to this subset. There exist several infrared-active out-of-plane vibrations, but in general such modes are weakly Raman active and are rigorously Raman forbidden for inversion symmetric molecules, such as *trans*-β-carotene.

The dynamical equations[10,12] are most easily written in terms of the planar cartesian coordinates of each atom, because the kinetic energy has then a diagonal form. In the valence-force approximation the poten-

(12) E. B. Wilson, Jr., J. C. Decius, and P. C. Cross, "Molecular Vibrations," McGraw Hill, New York, N. Y., 1955.

tial energy is initially expressed as a diagonal quadratic form in the internal dynamical coordinates corresponding to bond-length and bond-angle deformations. For each polyvinylene unit cell there are eight such coordinates, four stretches and four angular displacements (Figure 2), equal in number to the eight planar cartesian coordinates of the four atoms. Bond–bond, bond–angle, and angle–angle interactions are neglected. Such an approximation precludes the accurate numerical fitting of a complete vibrational spectrum; however, since the diagonal parameters all correspond to major interactions with obvious physical significance, the present approximate results tend to be meaningful. The presence of off-diagonal interactions can be related to the delocalization of the π-electron system. In particular, if the C=C and C—C spring constants are carried over from results on shorter molecules with a lesser extent of π-electron delocalization, the progressive delocalization with increasing length can be accounted for by the inclusion of off-diagonal terms in the force field. Alternatively, the effects of increased π-electron delocalization may be accounted for by an ad hoc progressive decrease of the C=C spring constant and a corresponding increase in the chain C—C spring constant. In the absence of a detailed theory,[11] which allows the deduction of all the spring constants from the electronic structure, the simplest approach seems to be warranted.

The internal coordinates $\rho(n,\varkappa)$ are readily expanded in terms of the Cartesian dynamic coordinates $u(l,j)$ by differentiating the projections of the instantaneous interatomic vectors with respect to the corresponding equilibrium bond directions and to the cosines of the equilibrium bond angles.[12] Here l or n enumerate the unit cell, j spans the set of atomic Cartesian in-plane coordinates within the lth unit cell, and $\varkappa$ is the set of internal coordinates within the nth unit cell

$$\rho(n,\varkappa) = \sum_{j}\sum_{k=-1}^{k=+1} D(r,\varkappa;n+k,j)u(l+k,i) \qquad (1)$$

The potential and kinetic energy are respectively

$$\begin{aligned} V &= \sum_{n,\varkappa}\lambda_{\varkappa}[\rho(n,\varkappa)]^2 \\ T &= \sum_{l,j} {}^1/_2 m_j[u(l,j)]^2 \end{aligned} \qquad (2)$$

where m_j is the mass of the atom of coordinates $u(l,j)$. In terms of Cartesian coordinates, V contains interactions between the nearest neighbor and next nearest neighbor unit cells. The Cartesian coordinates are renormalized in the usual manner

$$X(l,j) = \sqrt{m_j}u(l,j)$$

and, with the definition of the symmetrized dynamical matrix

$$H(l,j;n,k) = 2(m_j m_k)^{-1/2}\sum_{s,\nu}\lambda_{\nu}D(s,\nu;l,j)D(s,\nu;n,k)$$

the equations of motion become

$$\ddot{X}(l,j) = \sum_{n,k} H(l,j;n,k)X(n,k) \qquad (3)$$

$$j, k = 1 \ldots 8$$

For a general standing wave solution

$$X(l,i) = [X_c(j)\cos(qla) + X_s(j)\sin(qla)]e^{i\omega t} \qquad (4)$$

where a is the unit cell dimension along the chain axis, and $q = 2\pi/\lambda$ is the wave vector identifying a solution of wavelength λ. Equation 3 can be recast in a real Hermitian form suitable for computer diagonalization

$$\omega^2 X(J) = \sum_{K} H(J,K)X(K) \qquad (5)$$

with

$$X(J) = X_c(J) \qquad J = 1 \ldots 8$$

$$X(J) = X_s(J-8) \qquad J = 9 \ldots 16$$

$H(J,K) = \Sigma_{\sigma=-2}^{\sigma=2} H(l,J;l+\sigma,K)\cos(q\sigma a)$ for $J = (1 \ldots 8)$, $K = (1 \ldots 8)$ and $J = (9 \ldots 16)$, $K = (9 \ldots 16)$. $H(J,K) = \Sigma_{\sigma=-2}^{\sigma=2} H(l,J;l+\sigma,K-8)\sin(q\sigma a)$ for $J = (1 \ldots 8)$, $K = (9 \ldots 16)$. $H(K,J) = H(J,K)$ being independent of l, due to the periodicity of the chain.

A Jacoby diagonalization subroutine was used to determine the eigenvalues and cartesian eigenvectors, $X(J)$, for a set of values of $0 \leq q \leq \pi/a$ covering the first half of the Brillouin zone. In addition, by applying the transformation matrix to the cartesian eigenvectors the contribution of individual internal coordinates to the eigenvectors can be evaluated. These contributions are expressed in terms of squares of internal coordinate amplitudes, thereby eliminating phase factors (Table III). Each eigenvalue ω^2 corresponds to the square of an eigenfrequency and thus is doubly degenerate (in terms of running waves, oppositely propagating solutions $e^{i\omega t}$, $e^{-i\omega t}$ are degenerate). From the infinite set of modes of the infinite chain, corresponding to the continuum of q values, one has to select those congruent with the stationary modes of the finite conjugated chain in the real molecule. This is done by imposing suitable boundary conditions at two points delimiting a chain segment equal in length to the conjugated molecular backbone. These boundary conditions select a finite number of q values and also determine the ratio $X_c(j)/X_s(j)$ and should be chosen so as to correctly represent the effect of the terminal groups on the chain vibrations. For the molecules of interest here these groups are rather massive, for example, ionone rings or solvated polar end groups such as C=O. Thus, it seems reasonable to choose clamped boundary conditions, with the implications $X_c = 0$ and $N\lambda/2 = N\pi/q = L =$ the length of the conjugated chain. The fact that the Cartesian coordinates are defined in a frame which is not molecule fixed should, in an exact treatment, entail the appearance of two zero-frequency modes corresponding to rigid translations, whereas all other modes would leave the molecular center of mass stationary. For the infinite chain such conditions are automatically satisfied and the two zero-frequency modes, not shown in Table III, correspond to $q = 0$. For finite chains, even modes leave the center of mass stationary, because they are invariant under inversion. These are the only Raman-active modes of inversion symmetric molecules, *e. g.*, β-carotene. In the real finite chain, odd modes differ from those obtained from the infinite chain model in the displacement of atoms located near the chain extremities. These differences are more marked for the low q modes; in particular, the frquencies of the lowest q modes in the two lowest branches drop to zero. From the calculations we see, however, that in the frequency range of interest and for the chain

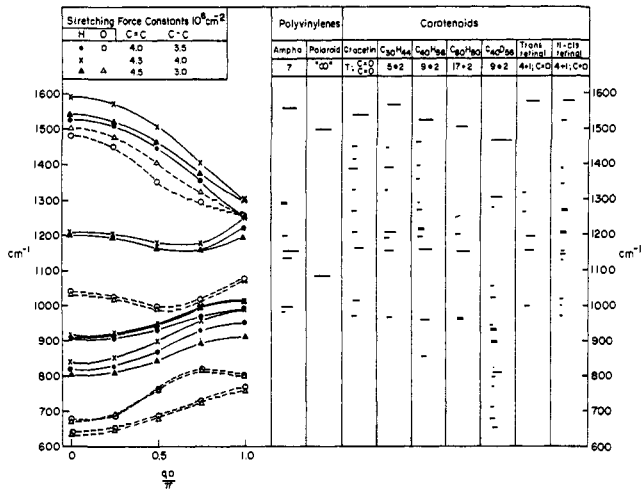

Figure 4. Dispersion curves computed for polyvinylene (left) and empirical Raman spectra (right). Force constants listed in Table I. Application to molecules requires a length-dependent variation of force constants. a is the length of the unit cell (Figure 2) and $\lambda = 2\pi/q$ is the wavelength of the vibrational mode. Modes in molecules are congruent with modes of infinite chain selected so that (integer)($\lambda/2$) = length of molecule. Right: polyvinylenes (a) Amphotericin B (Fungizone) has a straight segment of 7 conjugated bonds; (b) KN-42 Polaroid sheet has polyvinylene chromophors, some of "infinite" length,[8] ν(C=C) = 1495 cm^{-1}; carotenoids (c) crocetin, 7 conjugate bonds, two carbonyls. Compare with a. (d) Top: β-carotene homologs (2 bonds in the ionone rings), the last one having limiting long-chain properties (ν(C=C) = 1498 cm^{-1}, compare with b). (g) Deuterio-β-carotene. The computed bands do not account for the intense mode at 1303 cm^{-1}. Isomerization of *trans*-retinal into 11-*cis*-retinal results in splintering of the spectrum in the 1100–1400 cm^{-1} range.

lengths of the molecules under study, these effects are relatively small, so that the model represents satisfactorily the distribution of frequencies among the various types of vibrational modes, as expressed by the branches of the function $\omega = \omega(q)$. Figure 4 shows typical sets of eigenfrequencies calculated for three particular combinations of C=C and C—C stretching spring constants. All the spring constants are normalized to the mass of the H atom and yield the eigenvalues in units of reciprocal centimeters. Since the measured vibrational frequencies for a given transition do not vary among the protonated polyenes studied here by more than 15%, we chose for the initial calculation a set of parameters giving a set of frequencies within this 15% range. These parameters are essentially the same as those used by Popov and Kogan in their calculation for hexatriene[13] and are shown in Table I. Next the computer program was used to examine the sensitivity of eigenfrequencies to small change in the spring constants and to the doubling of the proton mass (deuteration) (Figure 4). These results can then be compared to experimentally observed variations in frequencies due to chain lengthening (which implies increased conjugation, *i.e.*, tendency toward equalization of the C=C and C—C spring constants), solvent-induced shifts, and effects of full deuteration. Such comparisons are important for substantiating the mode assignments, at least for the protonated molecules.

In general, the band-frequency assignments thus

(13) E. M. Popov and G. A. Kogan, *Opt. Spectrosc. (USSR)*, 17, 362 (1964).

Table I. In-Plane Force Constants for Polyvinylene (–CH=CH–)$_n$[a]

Notation PK[13]	Notation GR[11]	In-plane coordinate	Value in 10^5 cm^{-2}			
K_Q	Q_1	C=C stretch	4.0	4.5	4.5	5.0
K_{Q_0}	Q_2	C—C stretch	3.5	4.0	3.0	3.0
K_q	K_k	C—H stretch		4.0		
$H_{Q_0\alpha}$	H_β	H—C—C bend		0.75		
H_{Qq}		H—C—C bend		0.75		0.5
H_{Q_0Q}	H_γ	CCC bend		0.19		

[a] The stretching-force constants, already divided by the mass of the proton, are given in cm^{-2}. These force constants are equal to those given in mdyn Å^{-1} [12] multiplied by 1.69×10^5. (Multiplying this again by 2 gives the force constants of Popov and Kogan.[13]) The angular force constants, already divided by the proton mass and by the product of the lengths of the contiguous bonds, are given in cm^{-2}. This is the product of a force constant given in mdyn Å^{-1} [12] (or mdyn Å rad^{-2} [11]) multiplied by the aforementioned factor 1.69×10^5. The notations refer to the respective authors.

obtained are consistent with the assignments on the basis of the calculated contributions of the internal coordinates to the normal coordinates (Table III). For example, the ethylenic mode, shown by calculation to depend on C=C stretching, shows also a consistent decrease in frequency under conditions inducive to bond equalization. The calculation also shows that because of admixture, the contribution of C—C stretching is not unique to any normal mode, and therefore no increase of any particular vibrational frequency would be expected when C—C bonds are stiffened by bond equalization.

Experimental Procedures

1. Spectrometer. The Raman spectra were taken with a standard setup consisting of an ion laser, a double monochromator, and a photon counting system. The laser tube could be filled with either argon or krypton, thereby providing monochromatic excitation at one of 16 different frequencies, from the deep red (674.1 nm) to the purple (457.9 nm). The absorption of the laser radiation by the longer polyene molecules was high even in relatively dilute solutions and with far red excitation. Therefore, a nonpenetrating surface-scattering (reflection) geometry had to be used: the laser beam would impinge on the surface of a rectangular sample cell at an angle of incidence of the order of 60 to 70°, and the scattered radiation would be collected at 90° to the incident beam. The shorter carotenoid molecules offered more freedom of choice, because, in addition to the "reflection" spectra obtained with blue-green excitation as described above, good quality spectra excited by a penetrating beam could be obtained with yellow and red excitation. The concentrations of carotenoids ranged from 0.1 to 1.5 μM/l. of organic solvent. The latter was most commonly CCl_4, since it did not contribute Raman lines interfering with those of the pigments. (Spectra were also obtained in a large number of other solvents and they differed from those of the CCl_4 solutions by very small shifts which were specific to the solvents.) The signals were sufficiently strong so that there was no reason for cooling the photomultiplier; in some cases the spectra were plotted by a strip chart recorder fed from a digital counting system of variable integration time which was followed by a digital-to-analog convertor. Integration times were in the order of 0.1 to 0.5 sec at scan speeds of 50 or 100 cm^{-1}/min. In other cases the output of the pulse height discriminator was fed directly into a 1024 channel analyzer which was swept synchronously with the monochromator, at scan speeds ranging between 1 and 2.5 cm^{-1}/sec. The spectrum stored after a single scan was read out into an X-Y recorder, with no additional time constants in the circuit.

Absorption spectra were taken with a Cary 14 spectrophotometer. Solvent-induced shifts in λ_{max} agreed with the ones in the literature.[14]

(14) P. Karrer and E. Jucker, "Carotenoids," Elsevier, Amsterdam, 1950, Chapter 3.

2. Samples.[15] β-Carotene was purchased from Sigma. Another source of β-carotene, lutein, and the minor carotenoids was the extract of crushed spinach leaves, resolved into individual pigments by preparative tlc on silica gel.[16] The capsanthin samples consisted of the crude methanol extract of ground paprika. The absorption spectrum of the abstract was the bell-shaped curve characteristic of capsanthin and did not show the resolved vibronic structure of the β-carotene spectrum. The extract included much of the lipid fraction, and capsanthin itself presumably was ester linked to fatty acids. As these did not contribute to the resonance Raman spectrum, there was no need for further purification.

Crocetin and bixin were purchased from K & K Laboratories. Samples of the synthetic homologs of β-carotene were kindly supplied by Dr. W. Konig of BASF, 6700 Ludwigshafen, Federal Republic of Germany.

Samples of Amphotericin B (Fungizone) were kindly supplied by the Squibb Institute, New Brunswick, N. J. These samples were not dissolved but rather smeared on filter paper which was positioned in the reflection scattering geometry.

Deuterated algae (*Scenedesmus obliquus*)[17] were purchased in lyophilized form from Merck Sharp and Dohme.[18] Spectra were taken from individual pigments separated by tlc on silica gel, as well as from crude extracts. The tlc procedures were the ones described in the literature.[16,19]

Samples of a different kind were whole organisms and tissues, which yielded intense Raman spectra in the reflection configuration. These included practically any plant or animal tissue known to be rich in carotenoids[14] (*e.g.*, leaves, sections of shark liver, lyophilized deuterated whole algae).

Results

(a) As an example of a polyene chain having a well-defined length and being devoid of side methyl groups, we have measured the spectrum of the antibiotic drug Amphotericin B (Fungizone) (Table II).[9]

Table II. Resonance-Enhanced Raman Spectrum of the Polyene Segment of the Macrolide Antibiotic Amphotericin B (Fungizone)[a]

Amphothericin B (Fungizone)	
980	vw
995	s
1131	s, sh
1152	vs
1195	vw
1287	w
1554	vs
1597	vw
1624	w } carbonyl ?
1636	w }

[a] The sample was smeared on paper and the spectrum was taken in the reflection geometry with short integration time. Under these conditions the spectrum is wholly contributed by the polyene segment. The absence of a line at 1010 cm^{-1} distinguishes this polene from the carotenoids, which have methyl side groups.

The excitation was at λ 568.2 nm and the sample consisted of a streak of the powder smeared on filter paper. All the observable lines in the 900–1600 cm^{-1} region are ascribed to resonance-enhanced modes coupled to the conjugated chain. This is substantiated by the much lower intensity of the modes in the C–H stretch region (2800 to 3200 cm^{-1}). We should note the absence of a mode around 1010 cm^{-1}, which is present in all the isoprenoid chains and which hence can be assigned to the stretching of the $C-CH_3$ bond between the chain and side methyl carbon. The lines at 980 and 995 probably involve an admixture of γ(C=C—C) and β (C—C—H) angular deformations, the frequencies between 1130 and 1200 cm^{-1} belong to the admixed band of Q_0(C-C) and β(C–C–H), whereas the 1554 cm^{-1} line is the lowest permitted mode of the ethylenic band. The two lines at 1624 and 1636 cm^{-1} correspond to the carbonyl stretching band. Of course it should be remembered that all these modes are sufficiently admixed with Q(C=C) to ensure their resonance enhancement.

(b) β-Carotene and its synthetic homologs. The formulas of the homologs are given in Figure 3 and the spectra are shown in Figure 1. Again the Raman lines can be classified in the same three groups for all these molecules; the difference is that the C–C stretching mode of the side methyls with respect to the chain carbons is now evident at 1010 cm^{-1}. Figure 1 indicates that as the chain becomes progressively longer ν(C=C) decreases. The relative intensities of the bands in the 1150–1200 cm^{-1} region do change, but there is no monotonic upward frequency shift which would be expected for modes of pure Q_0(C–C) stretching.

(c) Natural carotenoids: crocetin, bixin, β-carotene, and capsanthin (Figures 1 and 3). The importance of crocetin and bixin (which are structurally distinct since they lack the terminating rings) is that their Raman spectra do not differ much from those of the other carotenoids. Thus the chain, which is common to all carotenoids including crocetin and bixin, is identified as the only contributor to the Raman spectra (there is no measurable contribution from the rings). This also is the reason why the gross features of the spectra of all the listed carotenoids are similar, irrespective of presence or absence of inversion symmetry due to identical or dissimilar end groups. Carbonyl or hydroxyl groups directly contiguous with the conjugated chain cause the lowering of ν(C=C), together with an appreciable red shift of λ_{max}.[14] The data in Figure 1 bear out the close similarity of the spectra of different C_{40} carotenoids. The search for features in the Raman spectra by means of which the C_{40} natural carotenoids, *e.g.*, lutein and zeaxanthin, the spectra of which are not reported here, could be distinguished requires the detailed examination of narrow spectral ranges. These results also explain why the Raman spectra scattered by intact plant tissues, when cursorily surveyed, are essentially identical with that of β-carotene.

(d) Deuterio carotenoids.[19] Figure 5 shows the spectrum of deuterio-β-carotene. The absence of a group of lines in the 1100 to 1200 cm^{-1} region and the apearance of a series of lines at much lower frequencies is qualitatively related to the theoretical result that the 1100 to 1200 cm^{-1} band involves strong admixtures of β(C–C–H) bending motions; the quantitative match between the model calculation and the experimental results is, however, much worse than for normal, protonated, carotenoids.

(e) Carotenoids in whole tissues. This part of the work was done in anticipation of using the mole-

(15) T. W. Goodwin, Ed., "Chemistry and Biochemistry of Plant Pigments," Academic Press, New York, N. Y., 1965, Chapters 3, 4, and 18.
(16) J. Sherma and G. S. Lippstone, *J. Chromatogr.*, 41, 220 (1969).
(17) W. Chorney, N. J. Scully, H. L. Crespi, and J. J. Katz, *Biochem. Biophys. Acta*, 37, 280 (1960).
(18) A. J. Williams, A. T. Morse, and R. S. Stuart, *Can. J. Microbiol.*, 12, 1167 (1966).
(19) H. H. Strain, M. R. Thomas, H. L. Crespi, and J. J. Katz, *Biochem. Biophys. Acta*, 52, 517 (1961).

Table III. Squares of the Eigenvector Elements Projecting the Normal Coordinates onto Some of the In-Plane Interval Coordinates[a]

	Internal					
	Q_1	Q_0	γ_1	γ_2	β_3	β_4
Normal	C=C	C—C	C=Ĉ—C	C—Ĉ=C	C—Ĉ—H	C=Ĉ—H
q = 0.2						
ν = 1553 cm^{-1}	0.12	0.025	0	0	0.29	0.27
1203	0.013	0.014	0.11	0.15	0.625	0.3
918	0.02	0	0	0	0.137	0.535
831	0	0.017	0.14	0.1	0.19	0.05
q = 1.0	0.12	0.015	0	0.015	0.325	0.35
ν = 1302 cm	0.12	0.015	0	0.015	0.325	0.35
1220	0	0.015	0	0.036	0.42	0.42
1017	0.04	0	0.075	0.05	0.36	0.19
953	0	0.027	0	0	0.141	0.195

[a] The normal coordinates are designated by the respective frequencies and momentum value q. The numbers measure the relative contribution of a deformation to a normal mode provided one does *not* compare stretching with bending deformations. The important conclusions are: (a) Q(C=C), the stretching deformation of C=C, has a predominant influence on the ethylenic mode at ~1500 and therefore the frequency ν(C=C) of this "ethylenic" mode is a reliable measure of the double bond stiffness; (b) no normal mode is distinguished by a unique contribution of Q_0(C—C).

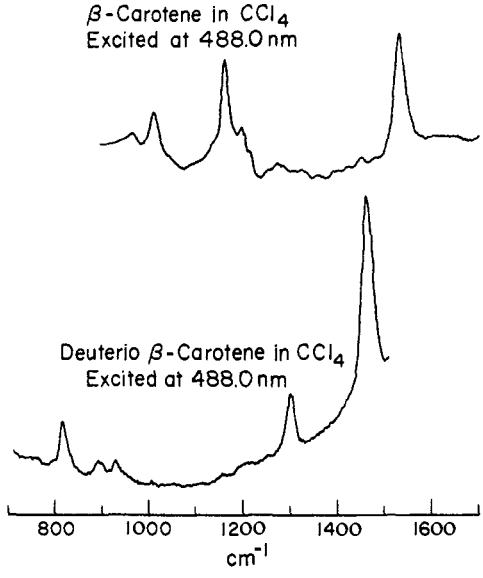

Figure 5. Raman spectrum of deuterio-β-carotene dissolved in CCl_4 and excited at 488.0 nm. All the observed lines are of the solute, while the doublet at 762 and 791 cm^{-1} of the CCl_4 solvent is barely noticed. The base-line slope may be the weak fluorescence of an impurity. The Raman spectrum of whole deuterated algae (*Scenedesmus obliquus*), which were shown by TLC to be richer in lutein than in β-carotene, is indistinguishable from the one shown here.

cules exhibiting resonance Raman effects as biophysical probes *in situ* (reporter groups). The most striking result of the runs is the apparent invariance of the spectra from sample to sample. The Raman spectra of purified β-carotene, lutein, and zeaxanthin are identical among themselves (±2 cm^{-1}) and the spectra of tissues rich in these pigments, individually or in a mixture, also look alike. The Raman spectra of lycopene and of capsanthin are distinguishable respectively from that of β-carotene *in vitro* and *in vivo*, but so are the absorption spectra.[14] It is likely that compound specificity and solvent specificity will be resolved when frequencies and line shapes are studied with a precision of 0.1 cm^{-1}.

Discussion and Conclusion

1. Relative Line Intensities and Selection Rules (also see ref 20). Three fundamental factors determine whether a given in-plane vibrational mode will be present in the Raman spectrum.

(a) For the inversion-symmetric molecules, only the even parity modes will be Raman active.[12] This type of mode assignment is usually checked by comparing Raman and ir spectra, since in the latter only the odd modes would be present. In practice, however, the in-plane modes of the conjugated chain are essentially nonpolar, their infrared activity is relatively weak, and, thus, the verification of ir activity is difficult.

(b) Since the observation of the Raman spectrum at low concentrations is made possible by resonance enhancement, which depends on the coupling of the vibrations to the π-electron system, and since there is very good evidence that bond alternation persists even in the longest of the polyene chains,[21,22] it is reasonable to assume that the strength of a given Raman mode is directly related to the contribution of the internal coordinate Q(C=C) to it. Using this criterion, the Raman-allowed modes subdivide into those which are strongly or weakly resonance enhanced, as indicated by the calculated contributions of C=C stretching into each of the modes (Table III). The weakness of the lines in the C—H stretch region and in the low-frequency region (below 500 cm^{-1}) provides qualitative experimental confirmation of this assignment.

(c) The strength of a given Raman transition will depend on its q value and on its position on the $\omega(q)$ dispersion curve. In particular, in a region of flat dispersion one expects a number of modes corresponding to different q values to contribute to the same Raman line (*i.e.*, have overlapping frequencies). This is clearly the case for the Q_0(C-C) + β(C-C-H) band in the 1150–1200 cm^{-1} region ($q \simeq 0.5$ to $q \simeq 0.8$). Superposition of modes is pronounced in the longer chains, where in a given interval of q values there are more modes than in the shorter chains. Even though the contribution of Q(C=C) to this band is relatively smaller than to the 1500-cm^{-1} band, the observed intensities may become comparable. In the spectra of the shorter chains (C_{30}, C_{35}, and retinal) the lines

(20) H. C. Longuet-Higgins and L. Salem, *Proc. Roy. Soc., Ser. A*, 251, 172 (1959).
(21) M. Tsuji, S. Huzinaga, and T. Hasino, *Rev. Mod. Phys.*, 32, 425 (1960).
(22) F. A. Savin and T. T. Sobel'man, *Opt. Spectrosc. (USSR)*, 7, 435 (1959).

in this frequency region are weaker and notably more split, probably because this band is quite sensitive to boundary effects, which are relatively more important for the shorter chains. This sensitivity of the 1200-cm^{-1} band to boundary effects may also well be related to its sensitivity to stereoisomerization.[7]

(d) In addition, the q value directly affects the Raman intensity because the wavelength $2\pi/q$ corresponding to q values allowed in carotenoid molecules is not completely negligible when compared with the radiation wavelength. This effect is independent of the resonance phenomenon and therefore can be discussed in classical terms. If the equilibrium atomic positions along the chain are defined by R_t, and the instantaneous positions by $R_t = R_{t0} + X_t$, the polarizability at a point r along a one-dimensional model molecule is given by $\alpha(r) = \alpha_0(r,R_{t0}) + \Sigma_t (\partial\alpha(r)/\partial R_{t0})X_t +$ higher order terms. First-order Raman scattering arises from the mode of wave vector q, $X_t = \sin qR_t$ in band σ, and will be proportional to

$$\alpha(r,\sigma,q) = \sum \frac{\partial\alpha(r)}{\partial R_t} \sin qR_t$$

and, if K is the momentum transferred between the incident and scattered light beams ($k_{\text{incident}} = k_{\text{scattered}} + K$, $K = k_{\text{incident}} \sin^2(\theta/2)$, θ being the scattering angle), the scattered field will be proportional to the spatial Fourier component

$$R(\sigma,\theta,K) = \int e^{-iKr}\alpha(r,\sigma,\theta)\mathrm{d}r$$

For scattering at 90° $K \simeq 0.5k_{\text{incident}} = (0.5 \times 2\pi)/\lambda \simeq 3/(5 \times 10^{-5})$ cm^{-1}, where $\lambda \simeq 500$ nm, the approximate wavelength of light in these experiments. Thus for the typical chain lengths of 15 to 30 Å the conditions $Kr \ll 1$ and $e^{-iKr} = 1 - iKr$ are always fulfilled. For genuine eigenmodes of a uniform chain that do not displace the molecular center of mass

$$R(\sigma,q,K) = -i\int Kr\sum_{R_i}(\partial\alpha(r)/\partial R_i) \sin qR_i\mathrm{d}r = \langle\partial\alpha(r)/\partial R_t\rangle_{\text{average}}\int_0^{Na} Kr \sin qr\mathrm{d}r$$

to a good approximation, where Na is the chain length.

$$\sum_{R_i}\partial\alpha(R)\partial R_t = \sum_i \delta(r - R_t)\langle\partial\alpha(r)/\partial R_t\rangle_{\text{average}}$$

Then replace Σ_t by $\int \mathrm{d}r$. Thus, the scattering efficiency, which is proportional to the square of the polarizability, will be proportional to

$$\left\langle \frac{\partial\alpha(r)}{\partial R_t} \right\rangle^2_{\text{average}} \frac{K^2N^2a^2}{q^2}$$

thus decreasing quadratically with the momentum q in the band.

Using these arguments, we assign the strong line that appears for all the carotenoids and retinals in the 1520–1600 cm^{-1} region to the smallest q vibration of the ethylenic band (see Table III). The strength of this transition may further be contributed to by the fact that in this low q region this band has a near-horizontal tangent and thus may represent the superposition of more than one mode. This contention is reinforced by the experimental results that the other transitions observed in the frequency region covered by this band, at least for the trans isomers, have relative intensities almost an order of magnitude weaker than predicted above.

2. Deuterated Carotenoids. The strongest line in the Raman spectra of deuterated β-carotene and lutein (Figure 5) is at 1462 cm^{-1} (β-carotene in CCl_4). The model calculation, as shown in Figure 3, indeed predicts the frequency of the ethylenic band in the correct region, once the same q value as for the normal molecule is assumed. $q = 2\pi/(Na)$ for the longest wavelength even mode where Na is the chain length, and $q_{\min} = \pi/a$ where a is the length of the unit cell. Thus $q/q_{\min} = 2/N = 2/11 \simeq 0.2$.

Table IV. Comparison of Raman and Infrared[19] Spectra of Deuterio-β-carotene

Ir	Raman	Ir	Raman
	1510 w		1023 w
	1463 vs		943 w
1305 s	1303 s		933 w
1164 m			898–906 w
1120 w	1128 w		818 s
1094 m			979 w
1086 m		765 s	767 w
1056 s	1053 w	726 s	
1047 s		708 s	710 w
			673 w
			652 w

For all the other lines, there is no correspondence between the calculated bands and the observed frequencies. More specifically, (1) the strong line at 1305 cm^{-1} has no analog of comparable strength within the ethylenic band of the trans-portonated carotenoids; (2) the frequencies of the lines at 820, 902, 912, and 955 cm^{-1} are much lower than predicted by the model for the Q_0(C–C), β(C–C–H) mixed band. These results imply that the simple theoretical model presented here is much less realistic for the deuterated carotenoids. Two explanations may be attempted. (1) Two (fundamental or combination) modes which were far apart in the protonated molecule may coalesce as a result of deuteration. This accidental degeneracy may enhance the interaction between the modes and cause their strong mutual repulsion (Fermi resonance),[23] an effect not accounted for by mere substitution of hydrogen masses. This model cannot explain the peak at 1303 cm^{-1} in deuterio carotenoids, because Fermi resonating modes appear in pairs. (2) Deuteration may induce a slight change in molecular configuration, more specifically, a change that enables some interaction between the in-plane chain modes and out-of-plane carbon bond angular deformations of proton–carbon bonds. This could explain the appearance of the strong line at 1305 cm^{-1} (which incidentally is also ir active) as an admixture between Q(C=C) and out-of-plane C—H bending and the lines between 820–1000 cm^{-1} as also admixed between the Q_0(C–C), β(C–C–H) in-plane band and some out-of-plane deformations. In this context, it should be mentioned that among the mono-cis retinal stereo isomers, the 11-cis is the one that has the most marked differences in its spectrum compared with the all-trans configura-

(23) G. Herzberg, "Molecular Spectra and Molecular Structure," Vol. II, Van Nostrand, Princeton, N. J., 1962, p 215.

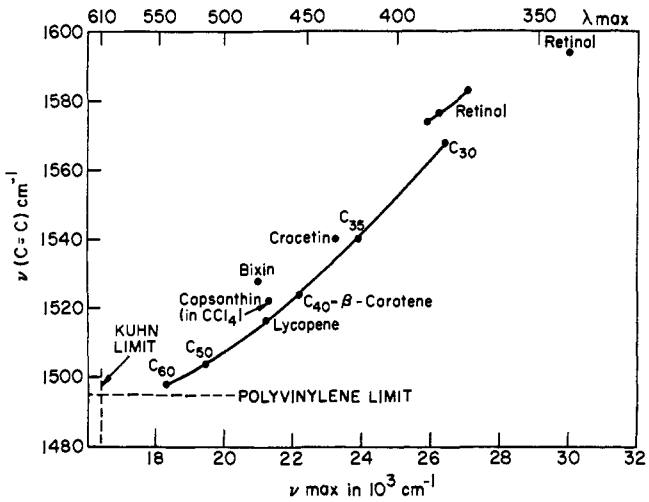

Figure 6. Correlation plot of ν(C=C) *vs.* $\nu_{max} = \lambda_{max}^{-1}$ in some natural and synthetic carotenoids. Each point summarizes a Raman measurement and an absorption measurement performed on the solution of a carotenoid in a particular solvent. The plot identifies the common cause of the two shifts in the π-electron delocalization (partial equalization of C=C and C—C bonds) by eliminating the particular mechanism inducing this effect. The major diagonal curve is the fixed solvent (CCl_4) locus of β-carotene and its synthetic hydrocarbon homologs; the locus correlates the length-dependent shifts (vinylene shifts) of the two observables; its curvature indicates that the approach of ν(C=C) to its long-chain limit is steeper than the respective trend of ν_{max}. The Kuhn limit[25] (lower left), extrapolating a semiempirical formula to infinite-chain length, is $\nu_{max} = 16.4 \times 10.3$ cm^{-1} (610 nm). The polyvinylene limit (lower left) of ν(C=C) for infinitely long chains was obtained from the Raman spectra of the multidisperse polyvinylene chromophors in a commercial KN-42 Polaroid dichroic sheet, excited at 674 nm, beyond the Kuhn limit.[8] The carboxylic carotenoids occupy a well-defined area on the plane. The plotting of fixed-solute loci, representing the shifts induced in one solute by different solvents, requires a degree of refinement not attempted in the present work.

tion, particularly in showing relatively strong lines in the 1300-cm^{-1} region and large perturbations in the Q_0(C–C), β(C–C–H) band. This is just a very tentative suggestion to explain the differences between normal and deuterated spectra; it may gain some support from the experimental observation that β-carotene and deuterio-β-carotene elute separately in certain types of chromatographic columns.[19]

3. Relationship between Vibrational and Electronic Spectra. The vibrational Raman spectra are an important source of new data for studying linear conjugated molecules. These molecules are favorite models for quantum chemical theories in which optical properties are correlated with structure. A zero-order free-electron theory, treating the polyene as a linear trough, predicts for very long polyene chains the equalization of carbon–carbon bonds and the coalescence of the conduction with the valence π-electron energy bands (black color, conductivity). In reality, one observes residual bond alternation[20,24] and a finite limit of $S_0 \rightarrow S_1$ energy gap in polyenes of increasing length.[25] The theoretical explanation of these interrelated properties is dependent on the fact that the number of π electrons in a polyene chain of n carbons is exactly n. The aufbau of the n electrons in single electron orbitals of a linear trough equal in length to the polyene molecule results in a highest occupied state having $n/2$ density maxima, congruent with the alternating bond pattern in the real molecule. The total charge distribution also exhibits the same periodicity for arbitrarily large n. When a corresponding periodic potential is introduced into the Schroedinger equation in a self-consistent manner (the Kuhn potential),[24] a finite $S_0 \rightarrow S_1$ energy gap ($= c\hbar/\lambda_{max}$) is obtained, which extrapolates to λ_{max} 610 mm for $n \rightarrow \infty$ (the Kuhn limit). Another prediction is that by inducing the admixture of excited π^* states into the highest occupied state, the periodicity of this potential will no longer be congruent with the polyene lattice, and bond alternation as well as the gap would tend to disappear. This limit of zero gap and no bond alternation is approached in the carbocyanine dyes, and a partial effect is evident in carbonylized carotenoids such as capsanthin, bixin, crocetin, and retinal. The outlined theory of color, which is an easily measurable property, is thus related to bond alternation, a difficult-to-measure structural property.[26]

Vibrational Raman spectra yield, when properly interpreted, the stretching constants for C=C and C—C bonds and thus produce direct information on the degree of bond alternation. The existence of the ethylenic mode in the vibrational spectrum is a qualitative indicator of the presence of bond alternation, and indeed, the mode as known in the polyene spectra is absent from the Raman spectra of carbocyanine dyes.

The correlation plot of the empirical ν(C=C) *vs.* λ_{max} or its inverse, ν_{max} (Figure 6), summarizes the relationships discussed above. The plot reveals π-electron delocalization as the common cause of the observed shifts both in λ_{max} and in ν(C=C) and summarizes a number of important observations.

Intermolecular polarization, induced by polar solvents, admixes excited states into the highest occupied state without changing the number of π electrons, and thus reduces the extent of bond alternation as it reduces ν_{max}. This is illustrated by the short section of data on retinal (Figure 6) taken in a number of solvents of varying degrees of polarity. Intramolecular polarization of the π system is encountered in carotenoids having a conbonyl group contiguous with the chain (*e.g.*, capsanthin, bixin, crocetin, retinal). When carbonylized carotenoids are compared with the parent hydrocarbons, one observes a remarkable degree of residual bond alternation accompanied by a relatively large drop in the $S_0 \rightarrow S_1$ energy gap.

The most conspicuous feature of the plot in Figure 6 is the correlation between ν(C=C) and ν_{max} through a progression of homologous polyenes of increasing lengths (vinylene shifts), when a common solvent is used for the whole sequence. The main properties of this fixed-solvent locus follow. (1) Marked downward shifts exist both in ν(C=C) and in ν_{max} in polyenes of increasing lengths. (2) In accordance with the model discussed above, both variables reach limiting values in long chains. The locus clearly indicates that ν(C=C) saturates in shorter chains before ν_{max} reaches its limiting value. The doubt as to whether the lowering of ν(C=C) reflects a genuine trend of electronic bond equalization or is just a sequential modification of the vibrational dynamics cannot be

(24) H. Kuhn, *J. Chem. Phys.*, 17, 1198 (1949).
(25) J. R. Platt in "Radiation Biology," A. Hollaender, Ed., McGraw-Hill, New York, N. Y., 1953.
(26) C. Sterling, *Acta Crystallogr.*, 17, 1224 (1964).

inequivocally resolved by vibrational analysis.[11] One may conclude, however, from data on molecules of constant length dissolved in solvents differing in polarity[27] (*e.g.*, retinal, Figure 6) that electronic bond equalization contributes appreciably to length-dependent shifts in ν(C=C).

The fact that the downshift of ν(C=C) levels off earlier in the sequence than does ν_{max} is the corollary of general principles. Two nondegenerate, close-in-energy eigenstates of an unperturbed (*e.g.*, vibrational) Hamiltonian would be repelled by the presence of an additional perturbation connecting these two states. (This is how the perturbing Kuhn potential repels the S_1 state from the S_0 electronic state of the linear trough.) Carrying the analogy to an idealized case of molecular vibration, a mode dominated by C=C stretching (*e.g.*, the ethylenic mode) would tend to coalesce with a mode dominated by C–C stretching when these two types of bonds tend to equalize. The off-diagonal terms in the vibrational Hamiltonian admix the internal coordinates and thus prevent the approach due to bond equalization of the ethylenic toward the C–C stretching modes which would be expected from progressive bond equalization. Thus the Raman spectra of long-chain polyenes indicate a higher degree of apparent bond alternation than that inferred from ν_{max} of the absorption spectra.

(27) M. E. Heyde, D. Gill, R. G. Kilponen, and L. Rimai, *J. Amer. Chem. Soc.*, 93, 6776 (1971).

Acknowledgments. We are indebted to R. G. Kilponen for taking the spectra, to Dr. König of BASF, 6700 Ludwigshafen, FDR, for the samples of β-carotene homologs, and to D. O'Brian from E. R. Squibb & Sons, Inc.

Solid-Phase Synthesis of Selectively Protected Peptides for Use as Building Units in the Solid-Phase Synthesis of Large Molecules

Moira A. Barton,* R. U. Lemieux, and J. Y. Savoie

Contribution from the Department of Immunology and the Department of Chemistry, University of Alberta, Edmonton, Alberta, Canada. *Received December 13, 1972*

Abstract: Self-catalyzed transesterification with 2-dimethylaminoethanol at room temperature was found to be effective for the removal of a variety of protected peptides from the Merrifield resin after solid-phase synthesis. The 2-dimethylaminoethyl function was removed from the resultant protected peptide esters by treatment with water at room temperature, to yield the corresponding protected peptide acids. The series of reactions comprising transesterification and ester hydrolysis was found to proceed with 0.3 ± 0.1% racemization of the C-terminal amino acid. The transesterification was found to be very slow when the peptide contained a C-terminal proline residue and in this case the reaction was expedited by the addition of thallium 2-dimethylaminoethoxide. *tert*-Butyloxycarbonylglycyl-L-alanine, prepared by the above methods, was utilized as a building unit in a further solid-phase synthesis using a variety of coupling procedures. The extent of racemization obtained in the coupling reaction was measured in each case. The highest yield and lowest degree of racemization was obtained using *N*-ethoxycarbonyl-2-ethoxy-1,2-dihydroquinoline as the coupling agent in dioxane solution. The procedures described herein were developed to provide a route for the solid-phase synthesis of selectively protected peptides which are required as building units for the solid-phase synthesis of large molecules.

The unequivocal chemical synthesis of proteins has long been a major goal of peptide chemistry and recent achievements in this direction are well known.[2-5] However, both solid-phase and solution methods of synthesis suffer from a number of disadvantages[6-14] when applied to large molecules, and it is evident that considerable modification of present techniques will be required before the synthesis of homogeneous proteins of defined structure can be readily accomplished.

It is possible that the major problems of the solid-phase method will be alleviated by the adoption of a fragment condensation strategy whereby the peptide chain will be assembled from a series of preformed protected peptide building units. The advantages of

(1) (a) This investigation was supported by grants from The Banting Research Foundation, The National Research Council of Canada, the Medical Research Council of Canada, and the University of Alberta Medical Research Fund. (b) Presented in part by M. A. Barton and R. U. Lemieux at the 14th Annual Meeting of the Canadian Federation of Biological Societies, Toronto, June 15–18, 1971, Abstract No. 35. (c) Abbreviations used are: Boc, *tert*-butyloxycarbonyl; Cbz, benzyloxycarbonyl; DMAE, 2-dimethylaminoethanol, DMF, *N*,*N*-dimethylformamide; EEDQ, *N*-ethoxycarbonyl-2-ethoxy-1,2-dihydroquinoline; DCC, *N*,*N*'-dicyclohexylcarbodiimide.

(2) (a) R. Hirschmann, R. F. Nutt, D. F. Veber, R. A. Vitali, S. L. Varga, T. A. Jacob, F. W. Holley, and R. G. Denkelwalter, *J. Amer. Chem. Soc.*, 91, 507 (1969); (b) R. Hirschmann, *Intra-Sci. Chem. Rep.*, 5, 203 (1971).

(3) B. Gutte and R. B. Merrifield, *J. Amer. Chem. Soc.*, 91, 501 (1969).

(4) B. Gutte and R. B. Merrifield, *J. Biol. Chem.*, 246, 1922 (1971).

(5) W. S. Hancock, D. J. Prescott, G. R. Marshall, and P. R. Vagelos, *J. Biol. Chem.*, 247, 6224 (1972).

(6) R. C. Sheppard, *Peptides, Proc. Eur. Symp., 11th, 1971*, in press.

(7) C. B. Anfinsen, *Biochem. J.*, 128, 737 (1972).

(8) E. Bayer, H. Eckstein, K. Hagele, W. A. Konig, W. Brunig, H. Hagenmaier, and W. Parr, *J. Amer. Chem. Soc.*, 92, 1735 (1970).

(9) A. Yaron and S. F. Schlossmann, *Biochemistry*, 7, 2673 (1968).

(10) M. A. Ondetti, A. Deer, J. T. Sheehan, J. Pluscec, and O. Kocy, *Biochemistry*, 7, 4069 (1968).

(11) J. Meienhofer, P. M. Jacobs, H. A. Godwin, and I. H. Rosenberg, *J. Org. Chem.*, 35, 4137 (1970).

(12) C. B. Anfinsen, *Pure Appl. Chem.*, 17, 461 (1969).

(13) F. C. Chou, R. K. Chawla, R. F. Kibler, and R. Shapira, *J. Amer. Chem. Soc.*, 93, 267 (1971).

(14) H. Hagenmaier, *Tetrahedron Lett.*, 283 (1972).